

Precursor activity in bright long BATSE γ -Ray Bursts

Davide Lazzati^{1,2}

¹ *JILA, Campus Box 440, University of Colorado, Boulder, CO 80309-0440*

² *Institute of Astronomy, University of Cambridge, Madingley Road, Cambridge CB3 0HA, England*

e-mail: lazzati@quixote.colorado.edu

11 June 2018

ABSTRACT

We study a sample of bright long BATSE GRB light curves in the 200 s before the detection of the GRB prompt emission. We find that in a sizable fraction of cases ($\sim 20\%$) there is evidence of emission above the background coming from the same direction of the GRB. This emission is characterised by a softer spectrum with respect to the main one and contains a small fraction (0.1 – 1%) of the total event counts. The precursors have typical delays of several tens of seconds extending (in few cases) up to 200 seconds (the limit of the investigated period). Their spectra are typically non-thermal power-law but for a few cases. Such long delays and the non-thermal origin of their spectra are hard to reconcile with any model for the progenitor.

Key words: gamma-ray: bursts — radiation mechanisms: non thermal

1 INTRODUCTION

In most Gamma-Ray Burst (GRB) models the main event is anticipated by a less intense emission, characterised by a thermal spectrum, called a precursor. Precursors can be distinguished into fireball precursors and progenitor precursors. The former are associated with the moment in which the fireball undergoes a transition from optical thickness to optical thinness (Paczynski 1986; Lyutikov & Usov 2000; Mészáros & Rees 2000; Daigne & Mochkovitch 2002; Lyutikov & Blandford 2004), while the latter are associated to the interaction of the jet with the progenitor star (especially in the context of massive star progenitors: Ramirez-Ruiz, MacFadyen & Lazzati 2002; Waxman & Meszaros 2003). The discovery of precursors, the understanding of their origin and the study of their properties would be of great importance to constrain the physics and some parameters of the burst outflow.

In the fireball precursor scenario, measuring the delay, duration, luminosity and typical frequency of the precursor would allow one to solve its properties and derive the Lorentz factor of the ejecta, their temperature at the transparency radius and the transparency and internal shock radii. All this parameters are extremely hard to measure otherwise. On the other hand, should a precursor be recognised as a progenitor precursor, its properties would give important constraints on the dynamics of the jet propagation in the progenitor and on the size of the progenitor star.

Observationally, little has been done so far. The main problem in identifying a precursor to a GRB lies in the definition itself of what a precursor is. As a matter of fact, defining a precursor implies defining a starting point of the

main emission different from “the first photon I see”. This problem has been addressed differently in the past by different authors. Koshut et al. (1995) defined precursors all the GRB pulses that had a peak intensity lower than that of the whole burst and were followed by a period of quiescence longer than the remaining burst active time. They searched the BATSE lightcurves for precursor activity and found that $\sim 3\%$ of all the BATSE GRB lightcurves showed signs of precursor activity. Their precursors were bright, containing a sizable fraction of the total event counts.

Since the precursors are theoretically predicted to be soft, another approach can be used with instruments sensitive in the keV range. In this case, it is possible to define a precursor as an emission episode that is present in the low-energy instrument but not in the high energy ones that are used to define the trigger of the main event. Soft precursors were detected with GINGA (GRB 900126: Murakami et al. 1991), HETE2 (GRB030329; Vanderspek et al. 2004) and *BeppoSAX* (GRB011121; Piro et al. in preparation). The GINGA precursor is the only one with a thermal spectrum, so that a comparison with theoretical expectations could be performed (Ramirez-Ruiz et al. 2002). The *BeppoSAX* and HETE2 precursors are both inconsistent with thermal emission and fitted successfully with a power-law.

In this paper, we perform a search for precursor activity in bright long BATSE GRB lightcurves, with a different approach with respect to Koshut et al. (1995). First, as a first condition to be considered precursor activity, an emission event must be detected *before* the GRB trigger. This is a somewhat instrumental definition, but since we are looking for weak precursors (theory predicts that precursors should contain a very small fraction of the burst energy), it turns

arXiv:astro-ph/0411753v2 21 Dec 2004

out to be an effective one. Second, we ask that the episode we call a precursor should decay in flux before the trigger. This choice is set in order to exclude slowly rising GRB emission from the precursor sample. We find, after rejecting some spurious events as background fluctuations, that many more GRBs are characterised by this kind of precursor activity ($\sim 20\%$ with respect to the $\sim 3\%$ of Koshut et al. 1995). We also find a-posteriori that our precursor definition is a good one, since these events have different properties than the main emission. Most of our precursors are characterised by non-thermal spectra and long delays, both properties being hard to reconcile with any model for their production.

This paper is organised as follows: in § 2 we describe the selection of our sample of GRB lightcurves; in § 3 we detail the data analysis and checks performed to build the precursor catalogue; in § 4 we describe the properties of the precursors and their relation to the properties of the main GRB and in § 5 we discuss our results.

2 SAMPLE SELECTION

The search was performed on a sub-sample of the BATSE GRB catalogue tailored to contain bright and energetic events, belonging to the sub-class of long-soft bursts. We selected therefore from the final BATSE GRB catalogue¹ all the events with duration $T_{90} \geq 5$ s, Fluence $\mathcal{F} \geq 1.62 \times 10^{-5}$ erg cm⁻² and 1.024 s integrated peak flux $F_{pk} \geq 3.2$ cts cm⁻² s⁻¹. We also excluded bursts that overlapped with either weaker or stronger bursts. This led to a sample of 146 bursts, 13 of which had to be rejected because of a non-continuous coverage of the light curve in the interval $t_{GRB} - 250 < t < t_{GRB} + T_{90}$, where t_{GRB} is the trigger time of the considered GRB. This led to a final sample of 133 GRB light curves.

3 DATA ANALYSIS

The search for precursor activity was performed in several steps. First, for each burst in the sample, the DISCLA continuous data file was retrieved from the archive². From the file, data for the 8 detector and the 4 channels were independently extracted for the interval $t_{GRB} - 300 < t < t_{GRB} + 1.5 T_{90}$, amounting to 32 light curves for each burst.

3.1 Detector Selection

The first step of the analysis is dedicated to the selection of the detectors more sensitive to photons coming from the direction of the considered GRB. To this goal, we first added together the 4 channels of each detectors, then performed a polynomial background fit to the 8 detectors individually and independently, generating the background subtracted light curve of each detector. We then computed the net counts of the burst in each detector and selected the detectors in which the GRB is brighter.

There was no fixed rule on the number of detectors. In

some cases a single detector was dominant, while in other cases the signal was dominated by four detectors. The subsequent analysis was performed on the summed data from the selected detectors. The selected number of detectors is reported in the second column of Tab. 2.

3.2 Wavelet detection

In this stage only data in the interval $t_{GRB} - 262.144 - \epsilon < t < t_{GRB} - \epsilon$ were considered, where ϵ is a small interval (usually 1 or 2 s) chosen in order to avoid a steep rise of the count-rate as the GRB trigger is approached. The number 262.144 is chosen in order to have 256 time bins of 1.024 seconds each (the resolution of the DISCLA data).

The issue is then to search for any emission component on top of a scarcely predictable variable background. This is a non trivial task, since the definition itself of emission exceeding a variable background is non straightforward. More so if we consider that the BATSE background in the soft channels (where we expect our precursor to be brighter) is known to suffer from non Poissonian noise (Connaughton 2002).

Giblin et al. (1999; see Connaughton 2002 for a full description) describe a procedure to estimate the background of the BATSE detectors at any given time. They adopt data from the satellite when it is positioned at the most similar geo-magnetic coordinates, i.e. 15 orbits (~ 84000 s) before and after the time of interest. They show that the average of the two rates gives a consistent estimate of the background rate at the time of interest, provided that: i) the data coverage is continuous in that interval; ii) there is no serendipitous source in the time intervals adopted for the background and iii) that the softest channel is not considered, since it is affected by unpredictable non-Poissonian noise.

We have tested this method and agree with the conclusions of Connaughton (2002), finding it not suitable for our analysis. On the one hand, it would lead to a further reduction of the sample due to the constraints above. On the other hand, it provides a good subtraction of the slowly evolving background in the soft channels, but not as accurate for the short time scale fluctuations, leaving therefore any potential contaminant to our search unaffected. We have therefore addressed the problem in a different way, adopting a detection algorithm which automatically corrects for slowly evolving background. This allows all the contaminants to be included in a first catalogue, which is then analysed to reject any source whose direction of arrival does not coincide with that of the GRB. We find a *posteriori* (see below) that this method is quite reliable, leading to a final version of the precursor catalogue with a low level of contamination.

The search for emission episodes in the selected time interval was performed with the use of a wavelet transform algorithm. Wavelet transform have multiple advantages with respect to sliding boxes in this case. Firstly, they perform an in-situ background subtraction, being insensitive to large-scale background variations. Secondly, they perform a multi-scale search, so that excesses are detected independently from their duration.

We adopted a reduction to one dimension of the two dimensional Mexican hat wavelet developed by Lazzati et al. (1999) for the analysis of ROSAT-HRI observations (Campana et al. 1999; Panzera et al. 2004). The wavelet mother

¹ <http://www.batse.msfc.nasa.gov/batse/grb/catalog/current/> see also Paciesas et al. (1999).

² <ftp://cossac.gsfc.nasa.gov/compton/data/batse/daily>

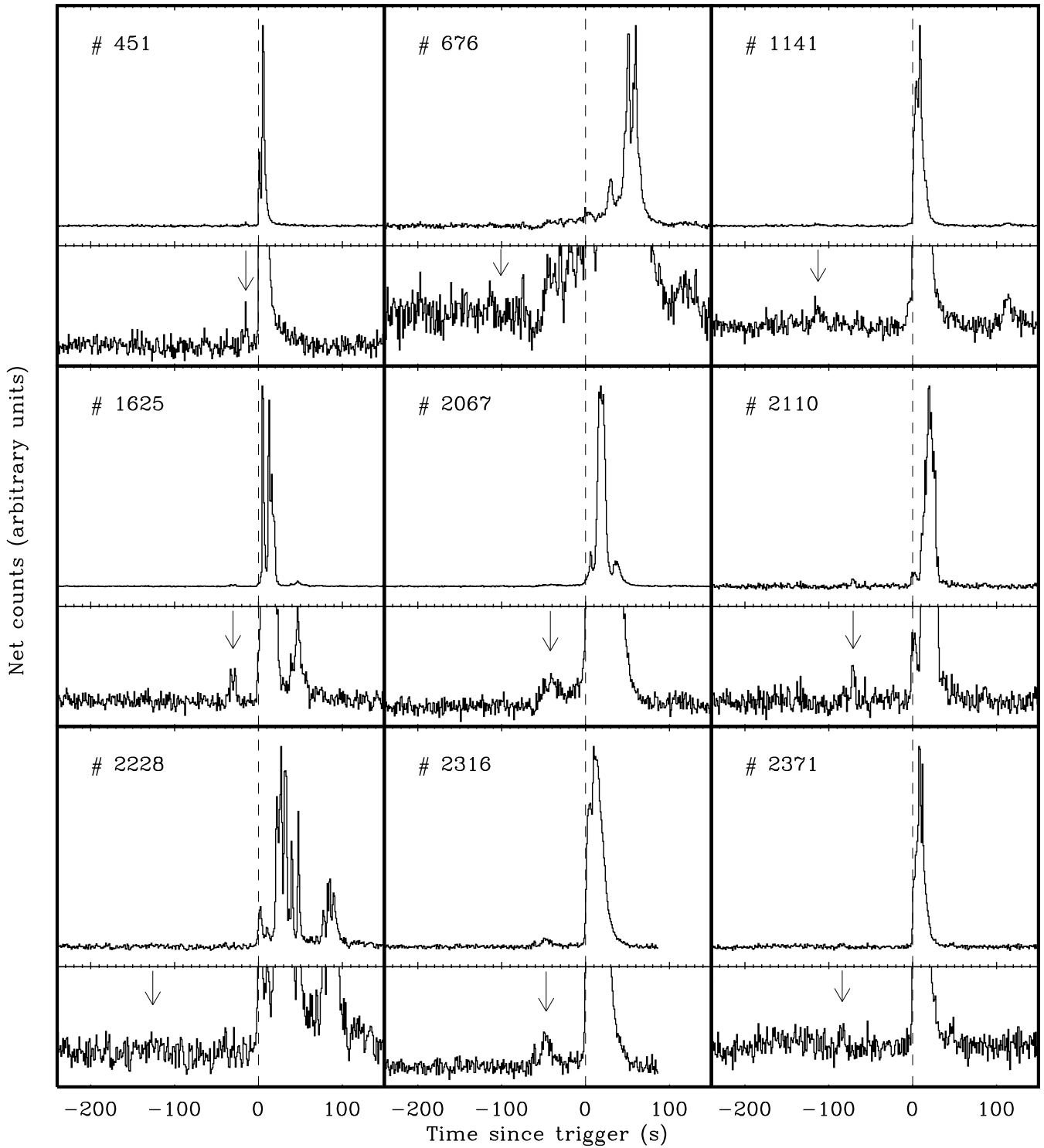


Figure 1. Atlas of the GRB lightcurves for which a precursor activity has been detected. For each GRB, in the upper panel the full light curve is shown, while in the lower panel the y-axis is zoomed in order to emphasise the precursor emission, indicated with arrow(s). The vertical dashed line shows the trigger time.

is built as the subtraction of two Gaussian, the negative one being wider by a factor $\sqrt{2}$. The time series is transformed and candidate sources are selected as peaks in the wavelet space at each scale in the time interval 200 seconds before the burst trigger. The statistical significance of candidate sources is assessed via simulations. For each burst, we sim-

ulate 10^4 mock Poissonian time series with the same large scale evolution (modelled with a polynomial function). We discard any peak in the WT of the real data which does not exceed the largest peak, in the same scale, of all the simulations, so that any candidate source has a probability $< 10^{-4}$ of being spurious. Finally, we cross correlate the cat-

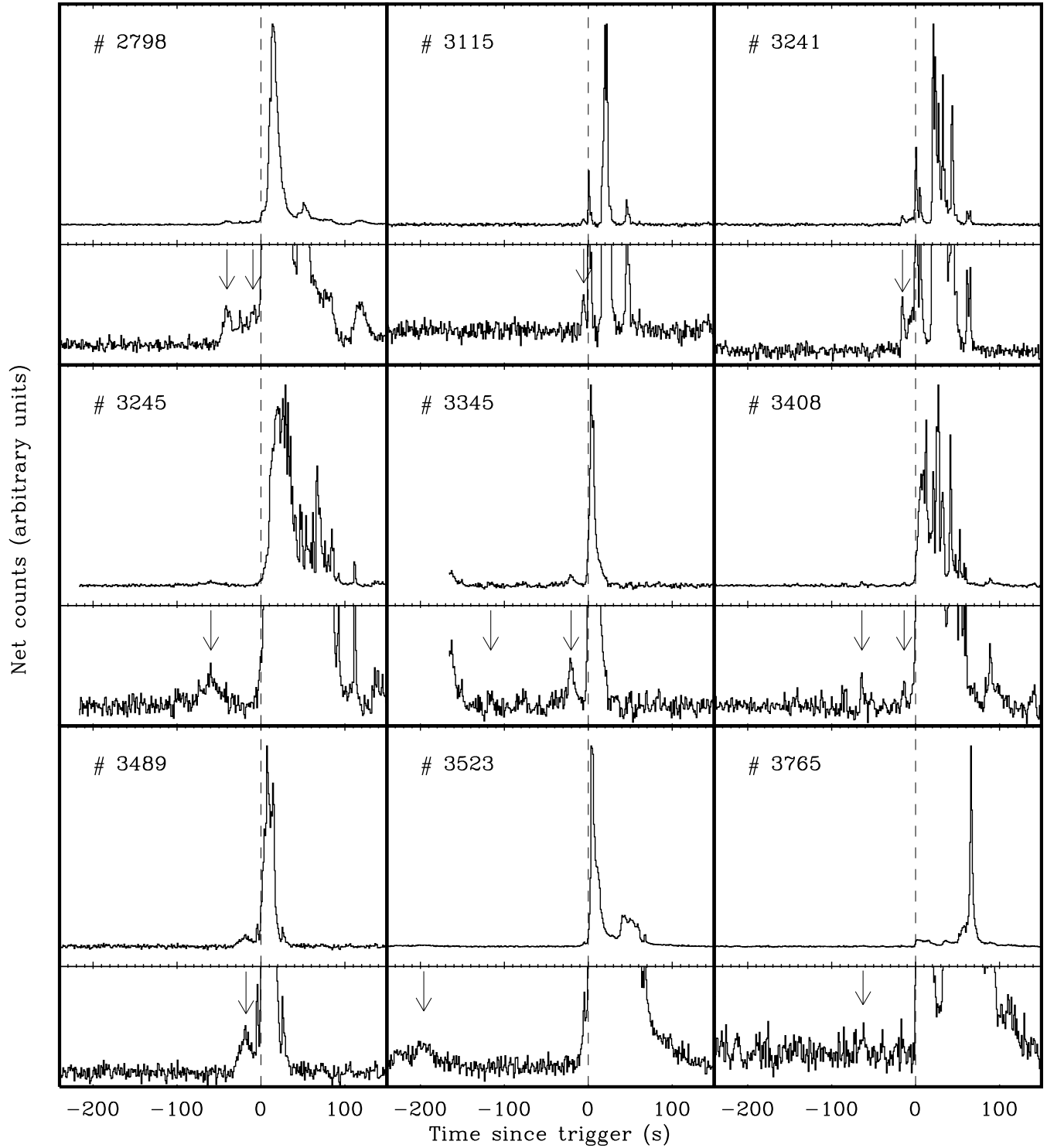


Figure 1. continued

alogue in order to get rid of sources detected simultaneously at different scales in the same position.

At this stage we are left with a catalogue of non-Poissonian excesses, characterised by a delay time from the GRB trigger and a rough estimate of their duration (the scale at which the source was detected at the highest signal to noise ratio). We cannot yet conclude that these are pre-

cursors associated to the forthcoming GRB emission, since we know that such non-Poissonian events are present in the BATSE detectors even without any association with a GRB. In order to rid the catalogue of spurious detections we compute the net counts of any candidate source in the 8 detectors independently. This was accomplished by fitting Gaussian functions to the excess. First, on the best signal-to-noise

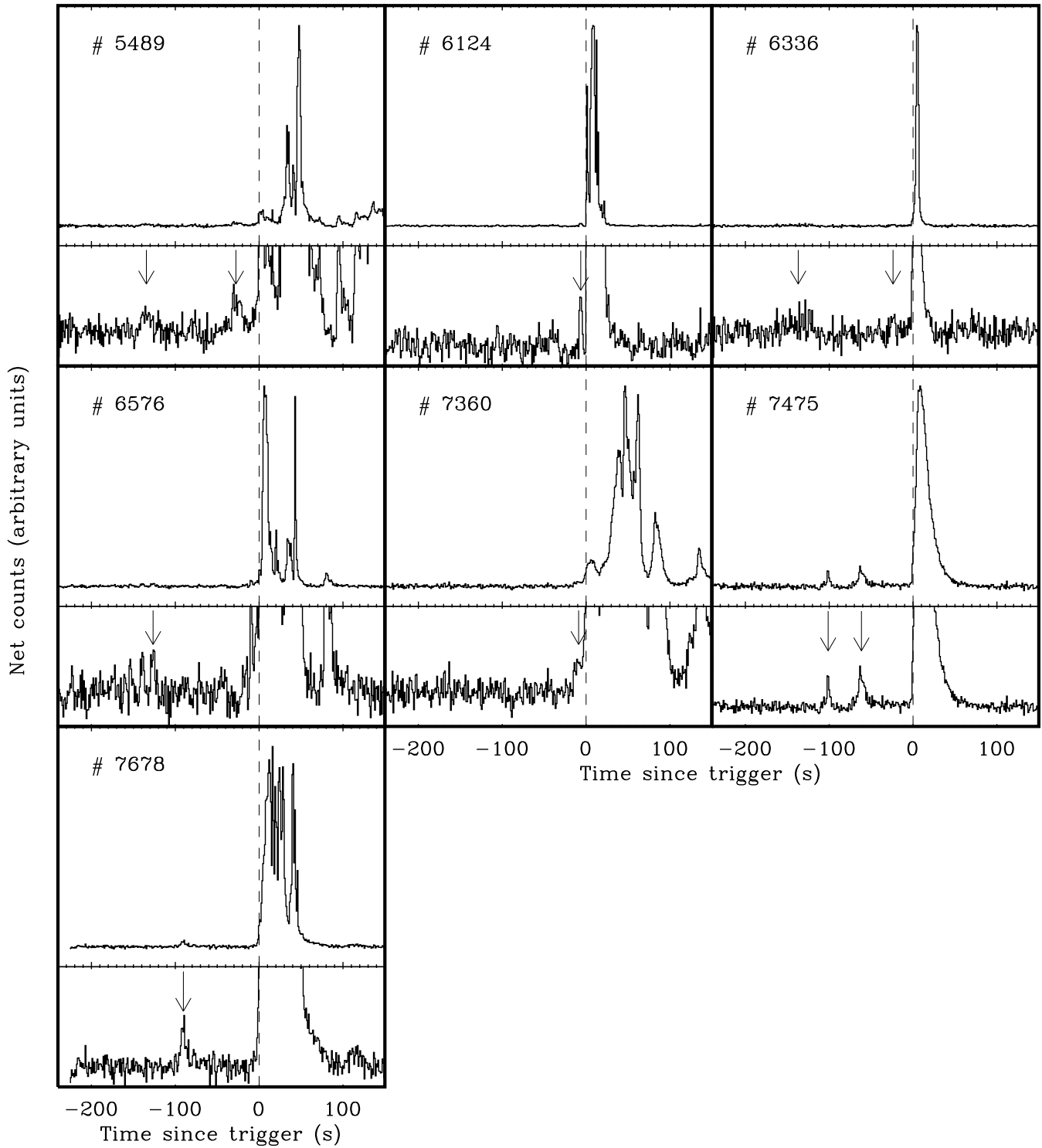


Figure 1. continued

detectors, the Gaussian is fitted with all parameters (centroid, width and normalisation) free, together with a third degree polynomial for the background modelling. Secondly, the same Gaussian, with fixed centroid and width, is fitted to the remaining detectors, leaving also the background free to adjust independently in each case. We then compare the relative counts of the candidate precursor in the different

detectors with those of the prompt GRB emission. If the relative ratios between the detectors (including upper limits) are in agreement, this means the candidate precursor emission comes from a direction in agreement with the direction from which the main GRB was detected. In statistical terms, in agreement means that the reduced $\chi^2 \leq 2$ and that no 3σ upper limit is violated. In this case the candidate precursor

Table 1. Summary of the detection and control analysis of the samples considered. Note that all the number of detections are for GRB, i.e. a burst with a multiple precursor counts only 1. On the other hand, since some bursts had both a confirmed precursor and a spurious one (based on the direction of arrival of the photons), the number of spurious plus confirmed detections is larger than that of total detections for the GRB sample. The average duration of spurious precursors (50 s) is longer than that of confirmed ones (10.7 s).

	GRB sample	Control Sample
Number of lightcurves	133	207
Number of detections/fraction	36/27%	22/11%
Number of spurious det./fraction	14/11%	22/11%
Number of confirmed det./fraction	25/19%	0/0%

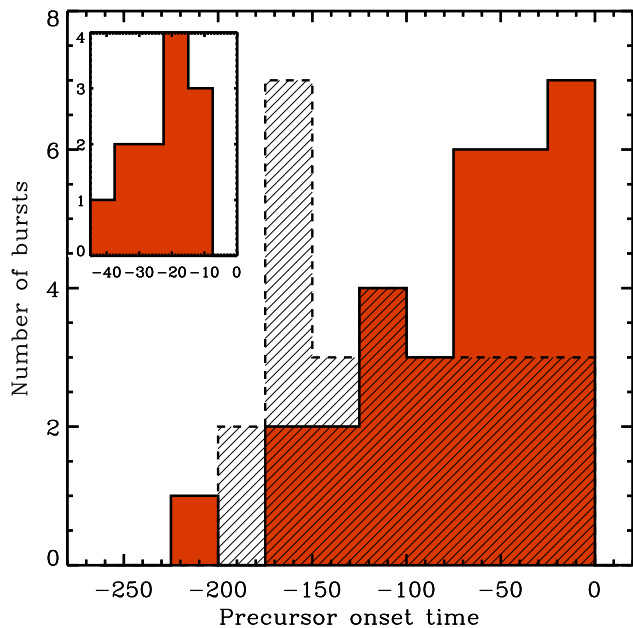


Figure 2. Distribution of the delays between the detected precursors and the trigger time of the prompt emission (filled histogram). The line filled histogram shows instead the distribution of the times at which spurious emission is detected in the control sample. The latter distribution is consistent with uniformity, while the true precursors are more likely to be detected close to the GRB. The inset show a higher resolution zoom of the distribution at small delays, emphasising the paucity of precursors with delays $\Delta t \leq 15$ s, very likely due to an incompleteness of our catalogue.

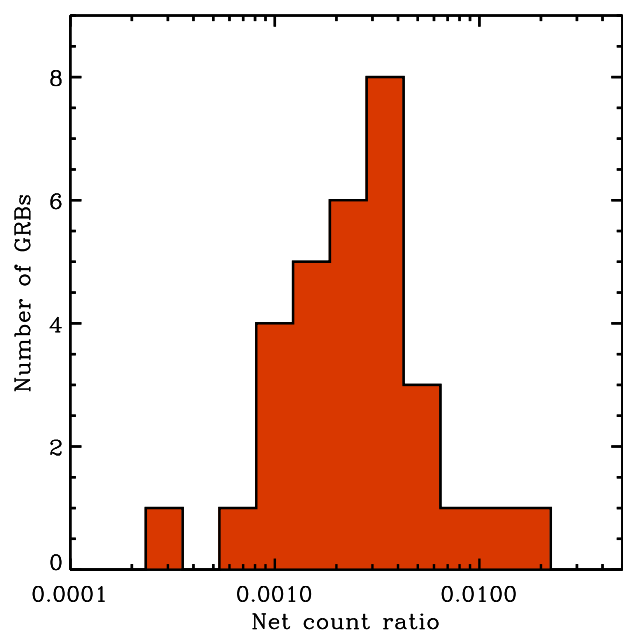


Figure 3. Distribution of the ratio of the precursor net counts over the main GRB net counts.

is elevated to the rank of confirmed precursor. Otherwise it is discarded. As it is summarised in Tab. 1, this procedure led us to identify 25 GRBs with precursors out of a contaminated catalogue of 36 GRBs with excesses. In 3 cases, the GRB showed both accepted and rejected episodes of emission. A word of caution should be spent for the possible biases of this technique. Since weak precursors have larger error bars, it's easier for them to be in agreement with the prompt emission relative counts and we expect therefore the contamination to be larger at small fluxes. This is however a problem of all catalogues: the closer is a source to the detection limit, the higher is the probability for it to be spurious. In addition, even if the test is performed on all the 8 detector, a GRB bright in only one detector will have a higher probability of a spurious precursor.

We still expect this catalogue to be contaminated to some level, since some precursors are detected only in few detectors (several even in a single one), so that the compar-

ison with the count ratios of the prompt is only indicative in these cases. To assess the level of contamination, we analysed a control sample of lightcurves, not associated to any known GRB emission, extracted from the DISCLA data 1 day before and 1 day after the analysed GRBs. We ended up with a control sample of 207 lightcurves, since all the cases in which the sampling of the interval was not continuous had to be discarded. These lightcurves were analysed in the same way as before, except for some inevitable differences. First, the number of detector where the analysis is performed, was randomly selected between 1 and 4, to mimic the first step of the procedure. Secondly, the detector ratios were not computed, since there is no ratio of the prompt emission to compare them to, and all the detected excesses are in this case known to be spurious.

We find that spurious non-Poissonian soft excesses are expected in 11% of the lightcurves, amounting to 14.6 expected excesses in our GRB sample. Reassuringly, this is

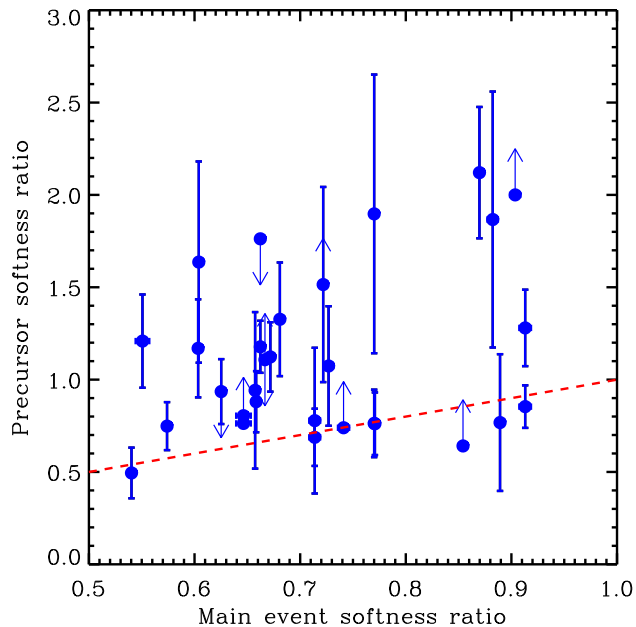


Figure 4. Softness ratio of the precursors vs. softness ratio of the main event. The softness ratio is defined as the ratio between the net counts in the first channel over the net counts in the second channel. The dashed line shows the locus of points where the two softness ratios are equal. All the precursors are consistent with being softer than the GRB to which they are associated.

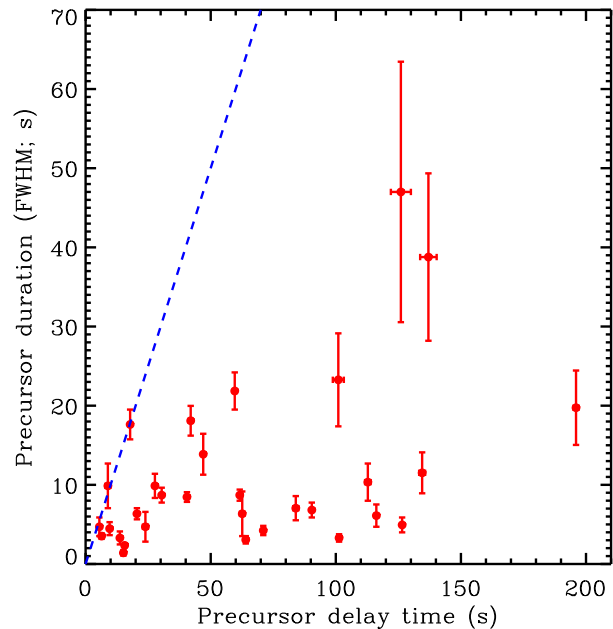


Figure 5. Duration of the precursors (FWHM) vs. delay time. Due to the adopted definition of precursor, all the points lay in the region where the delay is larger than the duration (the dashed line shows the duration equal delay condition).

exactly the number of excesses that were rejected in our analysis, confirming the goodness of our technique.

The resulting catalogue of precursors is detailed in Tab. 2. Additional tests on the reality of the 25 selected precursors are discussed below.

3.3 Characterisation

The characterisation of the detected precursors is performed by fitting Gaussian profiles to the data. Given the low signal-to-noise ratio of the sources, it is not possible to study their structure in further detail, and a symmetric fitting function like a Gaussian is always adequate. The width and centroid of the precursor is determined by fitting the highest signal-to-noise data, i.e. the sum of the first three channels of the brightest detectors (Sect. 3.1). The fit are always performed on the data without background subtraction. The background component is described by adding a 3rd degree polynomial to the Gaussian.

Extracting a spectrum from the BATSE LAD data for such faint sources is hopeless. We have therefore extracted a very-low resolution spectrum of the time-integrated precursor by re-normalising the four channel fluences of the main events, derived from the BATSE catalog, to the net-counts of the precursor. In this way we obtain a three point spectrum for most of the spectra. In the high energy channel the count-rate is always too low to yield any significant detection, so that only an upper limit can be obtained. In some cases also at softer energies the precursor is too weak to be detected. In these cases, when only two or less spectral points are available, we did not attempt to characterise the spectrum since any model can fit. Given the roughness with

which the three channel spectra are derived, we attempted only to fit power-laws and black body spectra. The model spectra were integrated in the broad energy bin before being fitted to the data. The statistical significance of the fit and the best model were evaluated by means of χ^2 statistics, see Tab. 2. All the uncertainties quoted in this paper are at the 1- σ level.

4 RESULTS

Table 2 reports the results of our search. We find precursor activity, in the 200 seconds preceding the GRB trigger, in 25 bursts out of 133 searched, for a total of 31 individual precursor events. Lightcurves of the bursts in which precursor activity has been detected are shown in Fig. 1. We conclude therefore that at least about 20% of the bright BATSE GRBs are characterised by a precursor activity to some extent. We say “at least” since, given the problems in the definition of a precursor (see Sect. 1), it is unavoidable that our search procedure misses some cases. As examples, consider a very bright precursor or a very small delay precursor (as predicted by theory). The former will trigger as a burst and will be excluded from our search, while the second will be mixed up with the main event, and therefore undetectable. This in addition to precursor events too weak to be detected.

The distribution of delay times of the detected precursors is shown with the filled histogram in Fig. 2. The onset time of the precursor is here defined as the centroid of the best fit Gaussian minus twice its σ . For comparison, with a line filled histogram, we show the distribution of the spuri-

Table 2. The catalogue of detected precursors. Each precursor is labelled with the BATSE trigger number of the main event to which is associated plus a letter *A* for the most significant event and *B* in case there is a second less significant precursor component.

ID	# of det.	Delay (s)	FWHM (s)	Fluence (10^{-8} erg cm^{-2})	Ratio ^(a) ($\times 10^{-3}$)	$\chi^2_{\nu}(PL)$	$\chi^2_{\nu}(BB)$	Spectrum ^(b)
451A	4	15.1 ± 0.2	1.4 ± 0.35	0.32 ± 0.1	1.53 ± 0.5	0.65	3.95	PL
676A	2	101 ± 2.2	23.3 ± 5.8	1.2 ± 0.3	2.8 ± 0.7	-	-	-
1141A	1	$113. \pm 1.1$	10.3 ± 2.3	1.3 ± 0.36	2.2 ± 0.6	-	-	-
1625A	2	30.4 ± 0.4	8.7 ± 1	4.3 ± 0.6	3.7 ± 0.5	2.83	3.22	NO
2067A	3	42 ± 0.8	18 ± 2	4.0 ± 0.5	4.5 ± 0.6	8.98	0.16	BB
2110A	3	$71 \pm .5$	4.2 ± 0.6	1.0 ± 0.2	2.5 ± 0.6	-	-	-
2228A	2	126 ± 4	47 ± 16	0.9 ± 0.4	3.1 ± 1.5	-	-	-
2316A	3	47 ± 0.5	14 ± 2.6	3.1 ± 0.8	5.8 ± 1.5	0.31	11.32	PL
2371A	2	84 ± 1	7.1 ± 1.5	0.4 ± 0.1	2.3 ± 0.7	-	-	-
2798A	3	40.5 ± 0.3	8.5 ± 0.6	4.6 ± 0.45	2 ± 0.2	25.5	0.37	BB
2798B	3	9.6 ± 0.5	4.5 ± 0.8	0.76 ± 0.26	0.33 ± 0.11	-	-	-
3115A	1	5.5 ± 0.4	4.7 ± 1.2	1.0 ± 0.2	3.8 ± 0.8	-	-	-
3241A	3	$15.6 \pm .2$	2.3 ± 0.2	1.2 ± 0.2	2.4 ± 0.3	-	-	-
3245A	2	59.6 ± 0.7	22 ± 2	9.2 ± 1.2	3.5 ± 0.5	0.29	21.4	PL
3345A	3	20.5 ± 0.3	6.3 ± 0.7	3.0 ± 0.4	9.3 ± 1.4	0.45	11.24	PL
3345B	3	116 ± 1	6.1 ± 1.4	1.3 ± 0.4	4.0 ± 1.2	0.01	2.28	PL
3408A	2	64 ± 0.2	3.0 ± 0.5	1.2 ± 0.2	1.1 ± 0.2	1.6	4.34	PL
3408B	2	13.7 ± 0.3	3.3 ± 0.8	0.6 ± 0.25	0.6 ± 0.25	1.3	11.73	PL
3489A	4	17.8 ± 0.6	17.7 ± 1.9	8 ± 1	16 ± 2	2.85	10.64	NO
3523A	2	196 ± 1	20 ± 5	$13. \pm 3$	3.3 ± 0.7	0.33	17.02	PL
3765A	2	62.6 ± 0.9	6.4 ± 2.8	0.5 ± 0.2	1.0 ± 0.4	0.05	2.77	PL
5489A	2	27.7 ± 0.7	10 ± 1.5	1.0 ± 0.2	2.0 ± 0.4	-	-	-
5489B	2	134.5 ± 1.2	11.5 ± 2.6	0.7 ± 0.2	1.3 ± 0.4	-	-	-
6124A	4	6.4 ± 0.15	3.5 ± 0.4	4.7 ± 0.6	4 ± 0.5	1.76	10.21	PL
6336A	2	137 ± 3	39 ± 10	6.0 ± 2.5	10 ± 4	-	-	-
6336B	2	24 ± 1	4.7 ± 1.9	0.8 ± 0.4	1.4 ± 0.7	-	-	-
6576A	3	126.5 ± 0.4	5 ± 1	0.8 ± 0.2	0.8 ± 0.2	0.96	11.95	PL
7360A	2	9 ± 1	10 ± 3	0.7 ± 0.2	1.2 ± 0.4	0.72	1.05	PL/BB
7475A	1	61.6 ± 0.25	8.7 ± 0.7	2.6 ± 0.3	4.9 ± 0.5	1.73	21.72	PL
7475B	1	101.3 ± 0.15	3.3 ± 0.5	0.9 ± 0.2	1.7 ± 0.3	1.19	14.23	PL
7678A	4	90.4 ± 0.4	6.8 ± 0.9	1.9 ± 0.4	1.6 ± 0.3	1.42	9.83	PL

^(a) Ratio between the main GRB emission and the precursor net counts in the whole BATSE sensitivity band.

^(b) Best fit spectral shape. PL=power law; BB=black body; NO=no model yielded an acceptable χ^2 ; - = not enough points for a meaningful fit.

ous precursors detected in the control sample. As expected, spurious detections are uniformly distributed in the whole interval, while the “real” precursors are more likely to be detected close to the trigger time of the GRB. The inset shows a higher resolution distribution for the small delay region, to underline the paucity of precursors with small time delay. As discussed above, this is likely to be due to an incompleteness of our catalogue rather than to a real paucity of cases. Nonetheless, it is surprising to note that the average delay time is of the order of several tens of seconds, while theory predicts delays of the order of few seconds at most, if not of a fraction of a second (see below).

Unfortunately no redshift information is known for the GRB sample where we perform the search and we cannot compute the energy that is contained in the precursors. We characterise therefore the energetics of the precursors through the ratio of their net counts to that of the main GRB to which they are associated. We should however keep in mind that the beaming of GRB and precursor photons may well be different. The distribution of this ratio is shown in Fig. 3. The precursors we detect contain on average a sizable fraction of a per cent of the total counts of the event. These precursors are therefore quite energetics especially if,

as predicted in some models, their beaming angle is wider than that of the main emission.

It may be argued that what we are detecting is not precursor activity but merely the beginning of the prompt emission. If we compare the count ratios in different channels this seems not to be the case. In Fig 4 we compare the softness ratio of the precursors with that of the integrated prompt emission. The softness ratio is here defined as the ratio of the first BATSE channel net counts over the second channel net counts. We find that all the precursors are softer than the time-integrated prompt emission. A similar softness (the dashed line in Fig. 4) has a vanishing probability of $P = 3 \times 10^{-6}$, and can therefore be rejected at about 5σ . This is in striking contradiction with what is expected from the hard-to-soft evolution usually found in GRB spectra (Ford et al. 1995; Frontera et al. 2000). Note again that we do not compare the precursor to the beginning of the burst, which is known to be particularly hard, but to the average softness. It seems therefore that the emission we single out before the burst is indeed something with a different origin.

In Fig. 5 we plot the duration (the full width at half maximum FWHM) of each precursor versus its delay time. Since we require a decrease in flux before the trigger in the precursor definition, all the points lay in the region of the

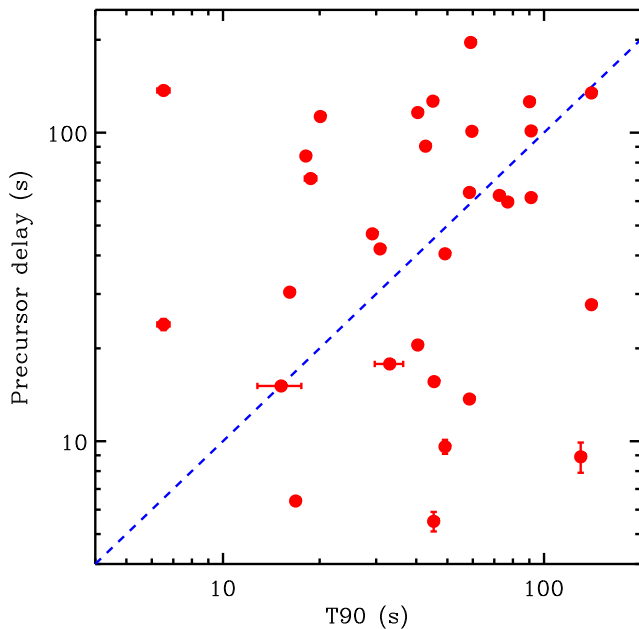


Figure 6. Precursor delay vs. duration of the main GRB emission. No correlation is apparent in the data. The correlation coefficient is $r = 0.082$.

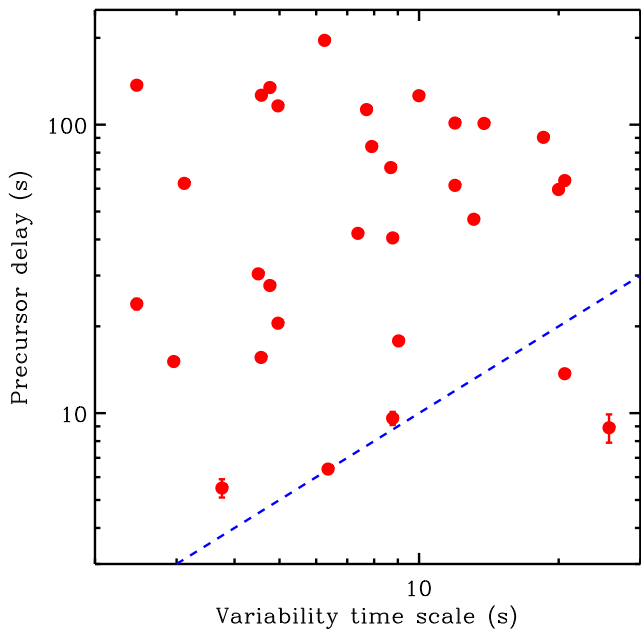


Figure 7. Precursor delay vs. variability time scale of the main GRB emission. No correlation is apparent in the data. The correlation coefficient is $r = 0.033$.

plot where the precursor FWHM is less than its delay. The dashed line shows the locus of points where the equality is realised. The comparison of this figure with Fig. 2 allows us to roughly estimate the number of lost precursors due to the above condition. Under the assumption that half of the precursors with duration < 20 s are lost (Fig. 5), we conclude that we miss ~ 9 precursors in our search (Fig. 2), increasing the fraction of GRBs with precursors to $\sim 25\%$. Of course, this estimate is based on the assumption, difficult to test in a robust way, that the lack of precursors with similar delay and duration longer than 20 seconds is a real effect and not a detection bias. This estimate should therefore be taken as tentative. To these, we shall add those missed due to their short delay (inset in Fig. 2), more difficult to quantify.

We now want to compare the properties of the precursors with those of the main event to see if any correlation exists. First, we compare in Fig. 6 the delay of the precursors with the burst duration (its T_{90}). In Fig. 7, instead, we compare the precursor delay with a measure of the burst variability time scale. We measure it as the half width of the auto-correlation function (following Boronovo 2004). In both figures, there appear to be no correlation whatsoever. This is confirmed by running statistical tests on the data.

In Figs. 8 and 9 we perform the same comparison but using the precursor duration (its FWHM) instead of its delay. Even though the small number statistics does not allow us to draw a definitive conclusion, it appears that the precursor duration is more closely correlated to the temporal properties of the main burst emission. In particular, there is only one case in which the precursor lasts more than the main emission.

5 DISCUSSION

We have analysed a sample of bright long BATSE GRB lightcurves to search for weak emission episodes taking place before the burst trigger or precursors. We define them as any count variation localised in time taking place before the burst trigger and coming from a location in the sky consistent with the direction of the main GRB event. This latter condition is verified through the consistency of the relative brightnesses of the burst and precursor in the eight BATSE detectors. We find that at least $\sim 20\%$ of the analysed bursts do have weak precursors. The precursors are weak, containing only a fraction of a per cent of the total counts of the event. Their properties do not correlate with the main event properties (as found also by Koshut et al. 1995; albeit under a largely different definition of precursor activity). We only find a mild correlation of the precursor duration (not its delay) with the burst T_{90} and its variability time scale.

Two important properties of the precursors are surprising. First their delay is long. Typical delays are of tens of seconds (see Fig. 2), but precursors with up to ~ 200 seconds delays are observed. If the precursor is associated in some way with the fireball initial release from the central compact object, and the γ -rays of the main GRB are released at a radius R_γ , at which the fireball has a Lorentz factor Γ_γ , we expect a delay:

$$\Delta t = \frac{R_\gamma}{2c\Gamma_\gamma^2} = 0.02 R_{\{\gamma;13\}} \Gamma_{\{\gamma;2\}}^{-1} \text{ s} \quad (1)$$

between the precursor onset and the trigger³. For standard internal shock parameters, the delay time is of the order of a fraction of a second. One may be tempted to vary the fiducial parameters in order to have a longer delay. This seems not to

³ Here and in the following we define any quantity $Q = 10^x Q_x$.

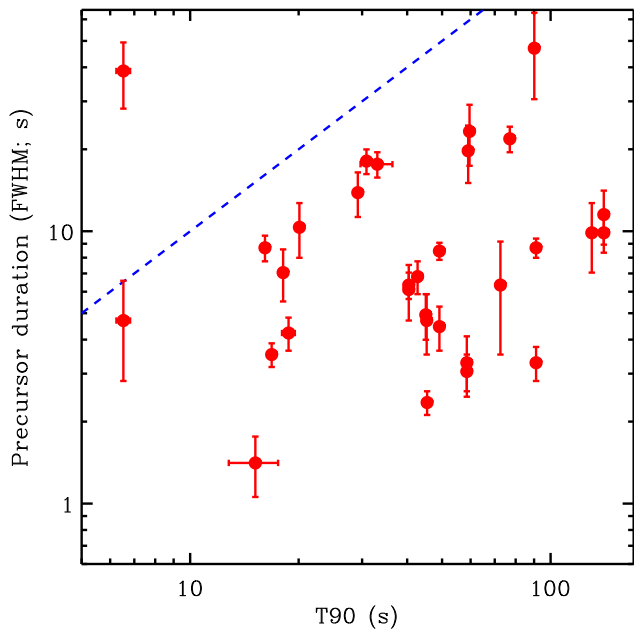


Figure 8. Precursor duration vs. duration of the main GRB emission. A mild correlation may be present, but it is not statistically compelling. The correlation coefficient is $r = 0.11$.

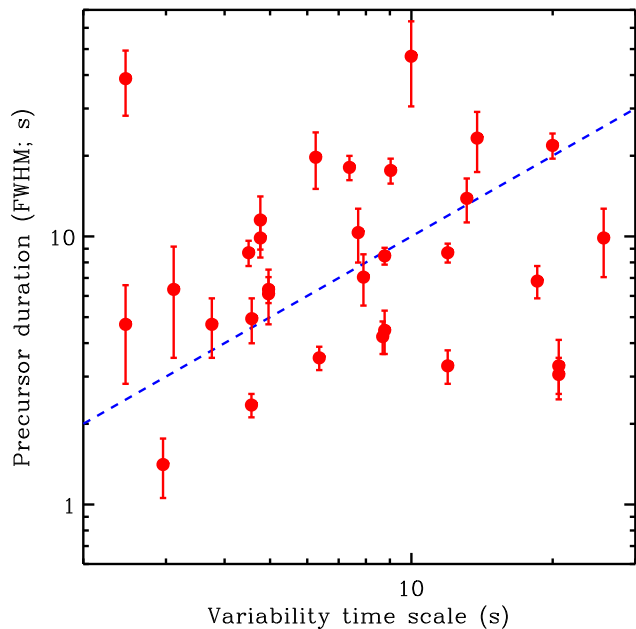


Figure 9. Precursor duration vs variability time scale of the main GRB emission. A mild correlation may be present, but it is not statistically compelling. The correlation coefficient is $r = 0.13$.

be the right way. As a matter of fact, a minimum variability time scale is associated to any radius and Lorentz factor by the curvature time scale (Fenimore et al. 1996):

$$t_{\text{var}} \geq t_{\text{curv}} = \frac{R_{\gamma}}{2c\Gamma_{\gamma}^2} = \Delta t \quad (2)$$

where t_{var} is the observed variability time scale. If the above interpretation for the delay were correct, we would therefore expect a relation $t_{\text{var}} \geq \Delta t$, in striking contradiction with the results of Fig. 7, which seems to underline an opposite relation.

If we consider progenitor precursors, i.e. precursors due to the interaction of the jet with its progenitor, we arrive to fairly similar conclusions. This is due to the fact that, again, the precursor is generated with the jet. There seem to be only two possible way out to this apparent contradiction. On the one hand, the curvature time scale may not apply. On the other, the precursor may be generated before the jet. In the first case, one would need to assume a fragmented fireball (Heinz & Begelman 1999; Dar & De Rujula 2000; 2004), or that the emission comes from localised spots (Lyutikov & Blandford 2004) in an otherwise continuous fireball. Also, an external shock onto a fragmented interstellar-medium may solve the variability problem (Dermer, Böttcher & Chiang 1999).

Alternatively, one may associate the precursor with something taking place before the jet is launched. In a binary merger scenario this may be associated to the first interaction of the binary system. In the hypernova scenario, it is harder to find any source of high energy emission before the jet is released, especially if we consider that the precursors have non-thermal spectra and must therefore be generated in an optically thin environment. A final possibility is that the first part of the jet, for some reasons that presently es-

cape our understanding, is not radiative and not produce GRB emission.

A second surprise, as anticipated, comes from the spectrum of the precursors. All the precursor activity that has been predicted in the various models is characterised by thermal spectra. In our sample of 19 precursors for which the data quality allowed a spectral characterisation, only two precursors are characterised by thermal emission, plus one with a dubious classification. In fact this is not a completely new issue, since two of the most well studied precursors, those of GRB 011121 (*BeppoSAX*; Piro et al. in preparation) and of GRB 030329 (*HETE2*; Vanderspek et al. 2004) are also characterised by non-thermal emission.

6 SUMMARY AND CONCLUSIONS

We have shown that a sizable fraction of bright GRBs are characterised by weak but significant precursor activity. These precursors have a delay time from the main GRB which is surprisingly long, especially if compared to the variability time scale of the burst itself. The precursor emission, contrary to model predictions, is characterised by a non-thermal spectrum, which indicates that relativistic electrons are present in the precursor emission region and that this region is optically thin. Unfortunately no redshift information is available for the GRB sample considered, so that it is not possible to estimate the energy involved in the precursor activity.

Future missions, such as *Swift*, will provide a large sample of GRB lightcurves with redshift where a similar precursor search can be performed. In addition, imaging capabilities will allow a more effective identification of activity related to the burst itself. This will allow us to gain a deeper

insight on these precursors and to exploit all their power in the understanding of the GRB phenomenon.

ACKNOWLEDGEMENTS

I thank Giancarlo Ghirlanda for useful discussions on the use of BATSE data and the anonymous referee for his/her useful comments. This research has made use of data obtained from the High Energy Astrophysics Science Archive Research Center (HEASARC), provided by NASA's Goddard Space Flight Center. This work was financially supported by the PPARC postdoctoral fellowship PPA/P/S/2001/00268.

REFERENCES

- Borgonovo L., 2004, *A&A*, 418, 487
 Campana S., Lazzati D., Panzera M. R., Tagliaferri G., 1999, *ApJ*, 524, 423
 Connaughton V., 2002, *ApJ*, 567, 1028
 Daigne F., Mochkovitch R., 2002, *MNRAS*, 336, 1271
 Dar A., De Rujula A., 2000, (astro-ph/0008474)
 Dar A., De Rujula A., 2004, *MNRAS* submitted (astro-ph/0308248)
 Dermer C. D., Böttcher M., Chiang J., 1999, *ApJ*, 515, L49
 Fenimore E. E., Madras C. D., Nayakshin S., 1996, *ApJ*, 473, 998
 Ford L. A., et al., 1995, *ApJ*, 439, 307
 Frontera F., et al., 2000, *ApJS*, 127, 59
 GIBLIN T. W., van Paradijs J., Kouveliotou C., Connaughton V., Wijers R. A. M. J., Briggs M. S., Preece R. D., Fishman G. J., 1999, *ApJ*, 524, L47
 Heinz S., Begelman M. C., 1999, *ApJ*, 527, L35
 Koshut T. M., Kouveliotou C., Paciesas W. S., van Paradijs J., Pendleton G. N., Briggs M. S., Fishman G. J., Meegan C. A., 1995, *ApJ*, 452, 145
 Lazzati D., Campana S., Rosati P., Panzera M. R., Tagliaferri G., 1999, *ApJ*, 524, 414
 Lyutikov M., Usov V. V., 2000, *ApJ*, 543, L129
 Lyutikov M., Blandford, R. D., 2004 (astro-ph/0312347)
 Mészáros P., Rees M. J., 2000, *ApJ*, 530, 292
 Murakami T., Inoue H., Nishimura J., van Paradijs J., Fenimore E. E., 1991, *Nature*, 350, 592
 Paciesas, W. S., et al., 1999, *ApJS*, 122, 465
 Paczynski B., 1986, *ApJ*, 308, L43
 Panzera M. R., Campana S., Covino S., Lazzati D., Mignani R. P., Moretti A., Tagliaferri G., 2003, *A&A*, 399, 351
 Ramirez-Ruiz E., MacFadyen A. I., Lazzati D., 2002, *MNRAS*, 331, 197
 Vanderspek R., et al., 2004, *ApJ* subm. (astro-ph/0401311)
 Waxman E., Mészáros P., 2003, *ApJ*, 584, 390